RSC Advances

ROYAL SOCIETY OF CHEMISTRY

www.rsc.org/advances

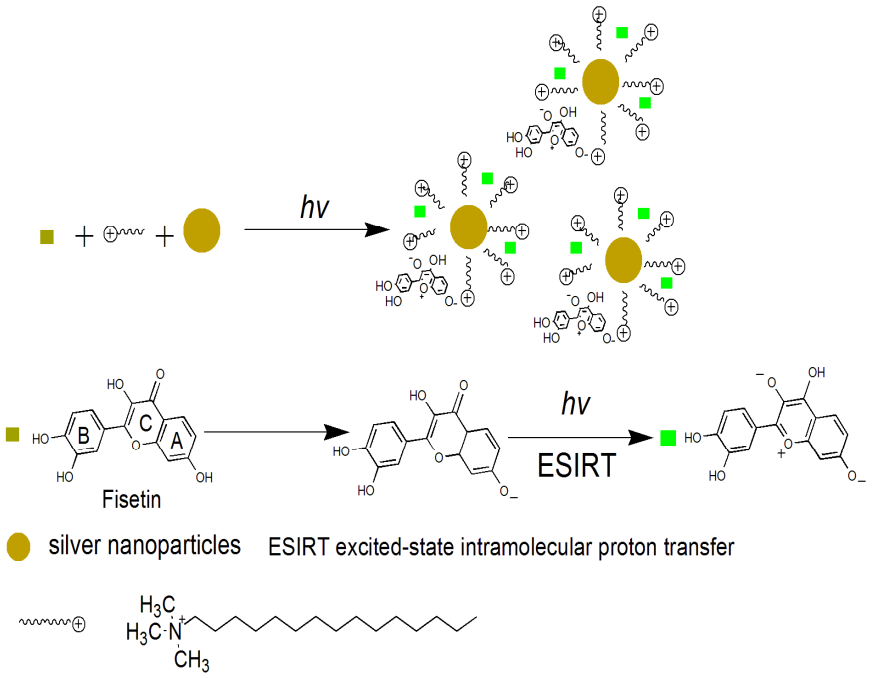

The synergies action of solubilization and sensitization of micelles and the metal-enhanced fluorescence of AgNPs enhance fluorescence of Fisetin.

Fluorescence enhancement of Fisetin by silver nanoparticles with cetyltrimethyl ammonium bromide micelles

Xiaodan Liu, Xia Wu*

Received (in XXX, XXX) Xth XXXXXXXXX 20XX, Accepted Xth XXXXXXXXX 20XX
DOI: 10.1039/b000000x

Abstract

In this paper, in situ synthesized cetyltrimethyl ammonium bromide micelles-capped silver nanoparticles were used to sensitively and directly detect Fisetin. Fisetin molecules solubilize in Stern layer of cetyltrimethyl ammonium bromide micelles and mainly bind to the head group of the micelles by electrostatic interaction and hydrophobic effect. Silver nanoparticles also solubilize in cetyltrimethyl ammonium bromide micelles and form the micelles-capped silver nanoparticles. The suitable distances between Fisetin molecules and silver nanoparticles for the fluorescence enhancement are provided by the micelles. The synergies action of the solubilization and sensitization of micelles and metal-enhanced fluorescence of silver nanoparticles promote the fluorescence enhancement of the system. Under optimized conditions, the fluorescence intensity of the system exhibits a linear response with the concentrations of Fisetin in range from 5.0×10^{-8} moL L^{-1} to 7.0×10^{-6} moL L^{-1} and the detection limit (*S/N = 3)* is 1.5×10^{-9} moL L^{-1}. Compared to the other methods, the developed method has higher sensitivity. And the method has been successfully used to detect Fisetin in actual samples.

Keywords: Metal-enhanced fluorescence; Fisetin; Silver nanoparticles; Cetyltrimethyl ammonium bromide.

Introduction

Silver nanoparticels (AgNPs) can enhance fluorescence response of fluorophores which are near the electromagnetic field of metal nanoparticles surface, and overcome the weak fluorescence of conventional fluorophores. The metal-enhanced fluorescence (MEF) of AgNPs has been widely used in fluorescent assays.[1,2] Many researches show that the MEF of AgNPs is not only relevant to their size and morphology but also to the distance between the fluorophore and the metal surface.[3,4] Lakowicz[5] reported that a suitable distance between the fluorophore and the surface of AgNPs favored the occurence of MEF. Nowadays, the suitable distance is usually adjusted by surface modification, hybrid and functionalization of AgNPs. Chen[6] used oligomer to control the separation distance of adjacent AgNPs, and developed two kinds of aptamer-modified AgNPs hybrid probes for the ultrasensitive determination of IgE. Ma[7] used Poly (3-acrylamidephenylboronic acid-co-acrylic acid) to adjust the distance between Ag core and porphyrin molecules, and proposed a core-shell AgNPs-based method to detect glucose. In this work, we used cation micelles to obtain the sutiable distance.

Fisetin (3,3',4',7-tetrahydroxyflavone) (Scheme-1), one of the flavonols, is found in eudicotyledons, vegetables, fruits, herbal and drinks.[8,9] Fisetin is a potent sirtuin-activating compound,[10] an agent that modulates sirtuins and plays important roles in anti-aging, anti-inflammatory, anti-prostate cancer, inhibiting human melanoma,[10-13] eutherapeutic for pancreatitis and diabetics[14]. Fisetin can also enhance the memory and may be good for treating memory disorders.[15] Therefore, the investigation for the determination of Fisetin is important for clinical medicine and pharmacology.[16,17] So far, many methods were used to detect Fisetin, including high performance liquid chromatography,[18,19] capillary electrophoresis [20] and electrochemistry.[21,22] But many methods have some disadvantages, such as time-consuming and tedious operation. So there is still an urgent demand to develop an accuracy, sensitivity, simplicity, fast response and low-cost method for the determination of Fisetin.

In this paper, in situ synthesized cetyltrimethyl ammonium bromide (CTAB) micelles capped-AgNPs were used for the sensitive and direct determination of Fisetin. Herein, the suitable distances for MEF between Fisetin molecules and the surface of AgNPs are provided by CTAB micelles. In addition, the interaction mechanism of the system is studied by resonance light scattering (RLS), fluorescence polarization, UV-vis spectrometry, Transmission Electronic Microscopy (TEM), dynamic light scattering (DLS), Raman spectra and Zeta potential etc.

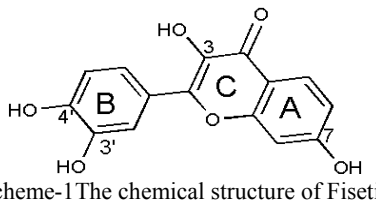

Scheme-1 The chemical structure of Fisetin

Experimental

Chemicals

The solutions of Fisetin, Kaempferol (Kae), Myricetin (Myr), Apigenin (Api) and Quercetin (Que), Galangin (Gal) and Luteolin (Lut) Morin (Mor) were prepared and all flavonoids were purchased from Alladin. Silver nanoparticles (1.0×10^{-3} moL L^{-1}) were synthesized by using chemical reduction method as described in the literature.[23]In this method, $AgNO_3$ (Sinopharm, China) was reduced by the trisodium citrate of 1% (Alladin, Shanghai). Silver colloid was formed until the colour of solution changed to pale yellow. The plasma resonance absorption peak of AgNPs is at 410 nm. The solution was stored in a refrigerator at 0 - 4 °C. Formic-NaOH buffer solution (pH=5.2) was prepared by diluting 1.8 mL of formic in 250 mL deionized water and adjusted using 0.2 moL L^{-1} NaOH.

All chemicals were of analytical reagent grade and ultra pure water was used throughout.

The strawberries were purchased from the local supermarket and crushed using a juice extractor, the fresh juice was centrifuged. The supernatant liquid was obtained and used for subsequent experiment.

Apparatus

Fluorescence and resonance spectra were carried out on an F-7000 spectrofluorimeter (Hitachi, Japan) using a 1 cm quartz cuvette. Fluorescence polarization was taken on a LS-55 spectrofluorimeter (Perkin-Elmer, USA). The absorption spectra were recorded using a U-4100 spectrophotometer (Hitachi, Japan). The TEM images were taken on a JEM-1011 Transmission Electron Microscope (JEOL, Japan). The pH was measured with a Delta 320-S pH-meter (Mettler Toledo, China). Surface tension experiments were performed on an automatic tensiometer JYW-200B (Dahua, China). Dynamic light scattering experiments were carried out on a BI 200-SM (Brookhaven Instruments, USA). Raman spectra were monitored using a QE 65000 (Ocean Optics, USA). The Zeta potential was tested in a Beckman Coulter Delsa Nano C Zeta-potential and particle size analyzer (Beckman Coulter, USA).

Procedure

Fluorescence spectra

The addition order of solution was 1.0 mL of 0.2 moL L^{-1} formic-NaOH buffer solution (pH = 5.2), 0.5 mL of 1.0×10^{-2} moL L^{-1} CTAB, 1.0 mL of 5.0×10^{-5} moL L^{-1} Fisetin and 1.0 mL of 4.0×10^{-5} moL L^{-1} AgNPs. The solution was diluted to 10 mL and maintained for 20 min. The fluorescence emission intensity at 545 nm was obtained using an excitation wavelength of 365 nm. The slit widths of excitation and emission were 10 nm and 2.5 nm, respectively. The scan speed was set at 240 nm min^{-1}. The enhanced fluorescence intensity of the AgNPs-CTAB-Fisetin system was calculated by using the expression $\Delta I_f = I_f - I_0$, where I_0 and I_f are the fluorescence intensity in the absence and presence of Fisetin, respectively.

Fluorescence polarization

The experimental conditions were the same as the section of

fluorescence spectra. The excitation wavelength was 365 nm and the fluorescence polarization intensity was measured at 545 nm. The excitation and emission slits were 10 nm and 5 nm, respectively. The fluorescence polarization (P) is defined as,

$$P = (I_{VV} + GI_{VH})/(I_{VV} + GI_{VH})$$

Where, I_{VV} and I_{VH} are the emitted fluorescence intensities parallel to and perpendicular to the polarizer of the exciting light. G ($=I_{HV}/I_{HH}$) is instrument correction factor.

Interference of other flavonoids and some ions

The measurement method was the same as "Fluorescence spectra" procedure. A certain amount of other flavonoids or metal ions were added in the system of AgNPs-CTAB-Fisetin, respectively.

Raman spectra

The laser excitation was set at 785 nm, the input laser source was 440 mW and the laser focus was 158 μm with 7.5 mm objective lens. The maximum laser power was 22 mW, the integration time of each spectrum was 1 s.

Dynamic light scattering

The size distribution was tested to use an argon laser (λ=532 nm) with variable intensity. The scattering angle was 90° with room temperature. The time of measurements was 60 s. The intensity autocorrelation data was used to calculate hydrodynamic diameter of silver nanoparticles.

Results and discussion

Fluorescence enhancement of Fisetin by AgNPs and CTAB micelles

Figure 1 displays the fluorescence spectra of the system. As seen from it, the fluorescence intensity of AgNPs-CTAB is the lowest. The fluorescence of Fisetin is weak and corresponding excitation and emission maximum wavelengths are at 370 nm and 480 nm, respectively. After CTAB was added, the fluorescence intensity of Fisetin significantly increases, and the emission peak shows a large red shift to 545 nm, the peak is attributed to the tautomer of Fisetin that arises from the excited-state intramolecular proton transfer (ESIPT) reaction.[24,25] Upon addition AgNPs to the CTAB-Fisetin system, the fluorescence intensity is further enhanced. The emission of the Fisetin tautomer has resonance coupling with surface plasmon of CTAB micelles-capped AgNPs, leading to larger fluorescence enhancement of the system. These results reveal that CTAB micelles and AgNPs have synergistic enhancement effect on the fluorescence intensity of Fisetin.

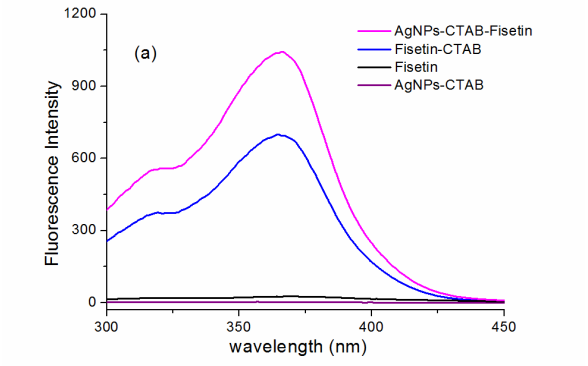

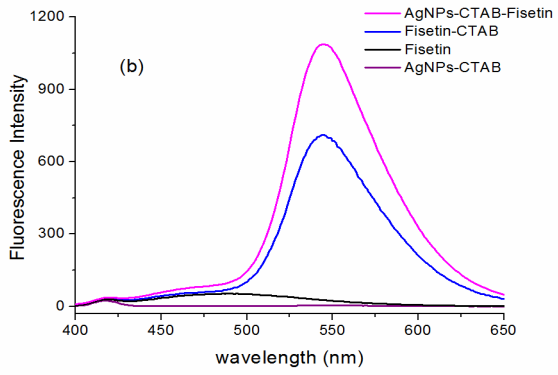

Fig. 1 Fluorescence spectra

(a) Excitation spectra (λem=545 nm) (b) Emission spectra (λex=365 nm) Conditions: $C_{Fisetin}$: 5.0 × 10^{-6} moL L^{-1}, C_{CTAB}: 5.0 × 10^{-4} moL L^{-1}, C_{AgNPs}: 4.0 × 10^{-6} moL L^{-1}, Formic-NaOH: 2.0 × 10^{-2} moL L^{-1} (pH=5.2)

Effect of experimental variables

Effect of pH and choice of buffer solution. Flavonoids with many hydroxyl groups can protonate and deprotonate in different acid and alkali medium. And their fluorescence intensities, peak positions and profiles are related to deprotonation of hydroxyl groups. The pH effect on the fluorescence intensity of the system was tested (Fig. S1, in the supporting information). The maximum enhanced fluorescence is at pH 5.2, the effect of different buffers on the fluorescence intensity shows that formic-NaOH is chosen for the following experiments. Further reasearches indicate the concentration of formic-NaOH buffer solution is 2.0 × 10^{-2} moL L^{-1}. The previous report[26] showed the pK_{a1} of Fisetin is 7.31 and the corresponding acidic OH group of Fisetin is 7-hydroxyl. In the selection conditions, 7-hydroxyl of Fisetin is deprotonation.

Effect of the concentration of AgNPs. AgNPs concentrations have a positive effect on fluorescence response (Fig. S2, in the supporting information). The fluorescence intensity of the system reaches maximum at 4.0×10^{-6} moL L^{-1}.

Effect of surfactants. A comparison of the effect of various surfactants on fluorescence intensity is tested (Fig. S3a, in the supporting information). As shown, CTAB gives the strongest synergistic fluorescence enhancement effect with AgNPs for Fisetin. The results indicate that the surfactants effect on the fluorescence enhancement of the system is not only relevant to the structures (tail length, head groups etc.) but also to the properties (CMC, electric, etc.) of the surfactants. In this work, CTAB is chosen as a sensitizer.

A plot of fluorescence intensity versus CTAB concentrations is performed (Fig. S3b, in the supporting information). When the concentration of CTAB is 5.0×10^{-4} moL L^{-1}, the synergistic fluorescence enhancement effect of CTAB and AgNPs is the strongest.

A surface tension concentration curve of CTAB is measured (Fig. S3c, in the supporting information). The critical micelle concentrations (CMC) of CTAB in the systems of Fisetin-CTAB, AgNPs-CTAB and AgNPs-CTAB-Fisetin are 7.0×10^{-4} moL L^{-1}, 3.1×10^{-4} moL L^{-1} and 3.3×10^{-4} moL L^{-1}, respectively. The CMC of CTAB is 9.0×10^{-4} moL L^{-1} in water.[27] We think AgNPs can promote the formation of the micelles at lower concentration of

CTAB. The CTAB concentration used in this paper is 5.0×10^{-4} moL L^{-1}, which is more than the CMC of this system. Here, CTAB forms micelles and the micelles provide a hydrophobic environment for Fisetin and reduce energy lose through collisions with other molecules. In addition, we think that AgNPs are capped by CTAB micelles, and a suitable distance between Fisetin and AgNPs is obtained for the coupling effect of oscillating dipole of the fluorescence of Fisetin and the plasmon resonance of AgNPs. That is the synergies action of the solubilization and sensitization of CTAB micelles and the MEF of AgNPs promote the fluorescence enhancement of the system.

The addition order and stability of system

The effect of the addition order on the fluorescence intensity was investigated. The result indicates that the best addition order of the reagents is formic-NaOH buffer solution, CTAB, Fisetin and AgNPs. Under the optimized conditions, the fluorescence intensity reached maximum after 20 min and remained stable for 2 h.

Selective fluorescence response of Fisetin

The effects of other flavonoids instead of Fisetin on the fluorescence response were carried out (Fig. 2). The results show that Fisetin gives the strongest fluorescence response. Fisetin is 3, 7-dihydroxy flavone, in contrast, 5, 7-dihydroxy flavones: Api and Lut give the smallest fluorescence response. While the fluorescence responses of the 3, 5, 7-trihydroxy flavones: Mor, Kae, Myr, Que and Gal are between 3, 7-dihydroxy flavones and 5, 7-dihydroxy flavones. This indicates that 3-hydroxyflavones have more efficient on excited-state intramolecular proton transfer than that of 5-hydroxyflavones in the system. From the literature we know,[20] micellar electrokinetic capillary chromatography was used to the selectivity of the separation of flavonoids due to surfactant micelles providing both ionic and hydrophobic sites of interaction. This means that the interaction between the flavonoids and the surfactant micelles is closely related to the structures of two entities. In this study, the selective fluorescence response of flavonoids should be attributed to the difference molecular structures of the flavonoids and the solubilization of flavonoids in CTAB micelles.

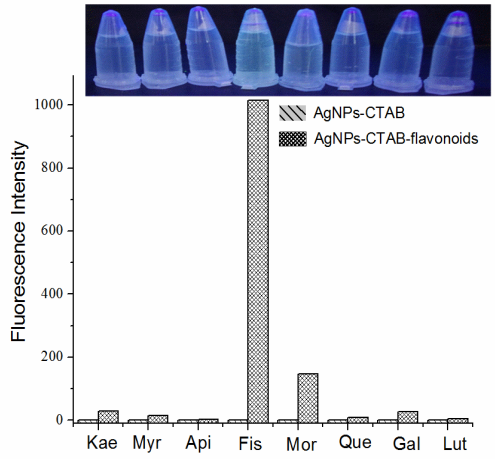

Fig.2 The fluorescence intensities of flavonoids

Conditions: $C_{Flavonoids}$: 5.0×10^{-6} moL L^{-1}, C_{CTAB}: 5.0×10^{-4} moL L^{-1}, C_{AgNPs}: 4.0×10^{-6} moL L^{-1}, Formic-NaOH: 2.0×10^{-2} moL L^{-1} (pH=5.2)

Interference of other flavonoids and some ions

The interferences of other flavonoids on the fluorescence of the system were tested. With 5.0×10^{-6} moL L^{-1} Fisetin, the maximum permissible molar excesses of other flavonoids causing a ±5% relative error in the fluorescence intensity was as follows: 10-folds molar excesses of Kae, Myr, Api and Que, 5-folds molar excesses of Gal and Lut 2.5-folds molar excesses of Mor. The interferences of some potentially coexistent ions on the fluorescence intensity of the system were also performed (Table 1). Most of the metal ions tested had little effect on the fluorescence intensity of the system within ± 5 % relative error.

Table 1 Interferences from foreign substances

Foreign substances	Concentration coexisting ($\times10^{-5}$ moL L^{-1})	Change of I_f (%)
Na^+, CO_3^{2-}	2.5	+3.6
K^+, Cl^-	2.5	+3.2
Ba^{2+}, Cl^-	2.5	+5.0
Al^{3+}, Cl^-	0.07	+4.4
Mg^{2+}, Cl^-	2.5	-3.4
Cu^{2+}, SO_4^{2-}	0.07	-4.0
Ca^{2+}, Cl^-	2.5	-2.9
Zn^{2+}, SO_4^{2-}	2.5	+4.4
Na^+, Cl^-	2.5	+4.8
Zn^{2+}, Cl^-	2.5	-4.0

Conditions: $C_{Fisetin}$: 5.0×10^{-6} moL L^{-1}, C_{CTAB}: 5.0×10^{-4} moL L^{-1}, C_{AgNPs}: 4.0×10^{-6} moL L^{-1}, Formic-NaOH: 2.0×10^{-2} moL L^{-1} (pH=5.2)

Analytical applications

Under the optimized conditions, a linear relationship (Fig.3) was obtained between ΔI_f and the concentrations of Fisetin in the range from 5.0×10^{-8} moL L^{-1} to 7.0×10^{-6} moL L^{-1}, with the correlation coefficient 0.998. The linear equation is $\Delta I_f = -7.37+2.66C$ (moL L^{-1}). The detection limit is 1.5×10^{-9} moL L^{-1}, according to the $3S_b/S$ criterion, where S is the slope for the range of the linearity and S_b is the standard deviation of the blank *(n=11)*. In comparison with other researches, the proposed method exhibits higher sensitivity. (Table 2)

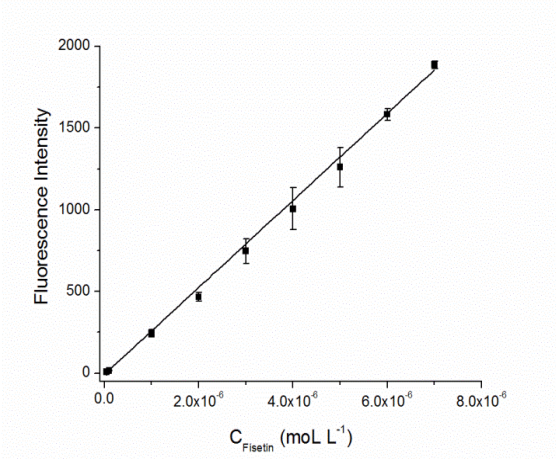

Fig.3 Calibration curve

Conditions:C_{AgNPs}:4.0×10^{-6} moL L^{-1}, C_{CTAB}:5.0×10^{-4} moL L^{-1}, Formic-NaOH:2.0×10^{-2} moL L^{-1}(pH=5.2)

Table 2 Comparison of some methods for the determination of Fisetin

Methods	material	Linear range	LOD[a]	References
Fluorescence	DNA abasic site aptamer	0.1-5.0 μM	50 nM	17
HPLC[b]-UV-vis		5.4–87μM	5.1μM	19
MEKC[c]	SDS[d] and ß-cyclodextrin	12-350 μM	3.0 μM	20
SWV[e]	Au-[f]BMI.PF_6 and	0.28-1.4 μM		
	[g]$Ni^{II}Ni^{II}$ complex	2.77-19.50 μM	50 nM	21
Fluorescence	AgNPs-CTAB	0.05-7.0 μM	1.5 nM	This work

[a]Limit of detection; [b]high-performance liquid chromatography; [c] micellar electrokinetic capillary chromatography; [d]sodium dodecyl sulfate; [e]square-wave voltammetry; [f]1-butyl-3-methylimidazolium hexafluorophosphate; [g][Ni_2(HBPPAMFF)μ-(OAc)$_2$(H_2O)]BPh_4

Determination of Fisetin in samples

The proposed method was used for the determination of Fisetin in samples. The amount of total flavonoids of strawberry juice was measured using the standard addition method, the measurement of average value (n=5) is 2.9×10^{-5} moL L^{-1}, the relative deviation is 5.9 %. The proposed method was also applied to detect Fisetin in a synthesis sample (1:10 mole ratio of Fisetin to Myr in 1000 times diluted strawberry juice) containing a suitable volume of strawberry juice, 1.0×10^{-7} moL L^{-1} Fisetin, and 1.0×10^{-6} moL L^{-1} Myr. The results were summarized in Table 3, the found values are identical with the expected ones and the recoveries are satisfactory. Hence, the proposed method is suitable for the determination of trace amount of Fisetin in strawberry juice.

Table 3 Determination results of Fisetin in 1000 times diluted strawberry juice

No.	Samples ($\times10^{-6}$moL L^{-1})	Fisetin Added ($\times10^{-7}$moL L^{-1})	Fisetin Found±SD ($\times10^{-7}$moL L^{-1})	Recovery (n=5, %)
1	Strawberry juice	1.0	0.99±0.032	99
2	Strawberry juice+Myr(1.0)	1.0	1.02±0.022	102

Interaction mechanism investigations

Figure 4 shows a comparison of resonance light scattering spectra. As seen from it, the RLS profile of Fisetin-AgNPs is different from the others. The RLS peak appears at about 425 nm, which should be attributed to Fisetin directly binding with AgNPs. The RLS peak intensity of AgNPs-CTAB-Fisetin is obviously higher than AgNPs-CTAB, but the shape and position of their peaks are similar. We speculate that Fisetin combines with AgNPs coated by CTAB micelles.

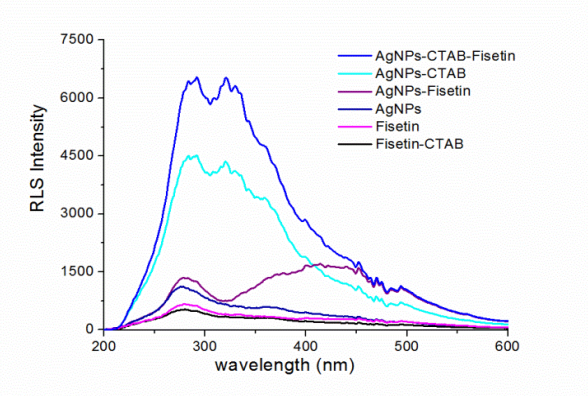

Fig. 4 Resonance light scattering spectra

Conditions: $C_{Fisetin}$: 5.0×10^{-6} moL L^{-1}, C_{CTAB}: 5.0×10^{-4} moL L^{-1}, C_{AgNPs}: 4.0×10^{-6} moL L^{-1}, Formic-NaOH : 2.0×10^{-2} moL L^{-1} (pH=5.2)

TEM images were used to verify CTAB micelles-capped AgNPs (Fig. 5). AgNPs are spherical shaped particles with average diameter of 15 nm (Fig. 5a). Silver nanoparticles are dispersed in the CTAB micelles (Fig. 5b). After addition of Fisetin, AgNPs distinctly aggregate and the diameter is about 50 nm (Fig. 5c). However, when CTAB, AgNPs and Fisetin coexist in the system, AgNPs disperse in CTAB micelles (Fig. 5d). The results confirm the formation of the micelles-capped AgNPs. We think that CTAB micelles provide the suitable distance between AgNPs and Fisetin, leading to the fluorescence enhancement of AgNPs-CTAB-Fisetin system.

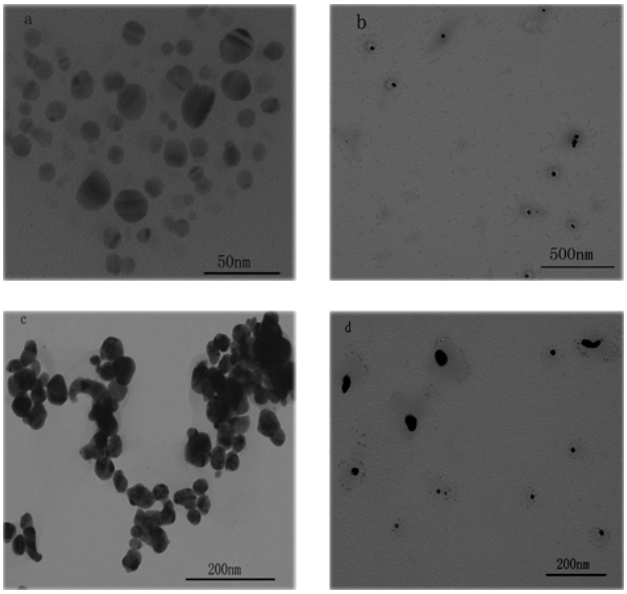

Fig. 5 TEM images of the system

(a)AgNPs, (b)AgNPs-CTAB, (c)AgNPs-Fisetin, (d) AgNPs-CTAB-Fisetin

Conditions: $C_{Fisetin}$: 1.3×10^{-4} moL L^{-1}, C_{AgNPs}: 1.0×10^{-4} moL L^{-1}, C_{CTAB}: 5.0×10^{-4} moL L^{-1}.

Dynamic light scattering (DLS) is alternative method for monitoring particles size. Unlike TEM giving the number-average diameter, DLS exhibits a hydrodynamic diameter[28] (Fig.S4, in the supporting information). DLS datum show that the average sizes of free AgNPs and AgNPs-CTAB are 74 nm and 92 nm, respectively. The increase particles size proves CTAB micelles coat on the surface of AgNPs, and AgNPs are well dispersion in CTAB micelles. AgNPs gather to 360 nm in the presence of Fisetin because Fisetin directly binds to AgNPs. The size distribution of AgNPs-CTAB-Fisetin is from 6.66 nm to

203.2 nm. According to the sizes distribution of AgNPs-CTAB and AgNPs-CTAB-Fisetin and TEM images (Fig. 5 b, d), we find that CTAB micelles are preferred to coat smaller sizes AgNPs. AgNPs that are approximate 10 nm maybe more effectively promote the fluorescence enhancement of the system.

Molecular rotational diffusion of the system was monitored by the fluorescence polarization (*P*). Under optimized conditions, the *P* values of CTAB-Fisetin and AgNPs-CTAB-Fisetin are 0.358 and 0.456, respectively. The result reveals that AgNPs can further hinder the rotational diffusion of Fisetin in CTAB micelles, leading to the decrease of rotation velocity of AgNPs-CTAB-Fisetin. This result further proves that Fisetin combines with AgNPs coated by CTAB micelles.

Surface-enhanced Raman scattering (SERS) was experimented for further verifying the interaction among AgNPs, Fisetin and CTAB (Fig. 6). Raman intensities of AgNPs-CTAB, Fisetin and Fisetin-CTAB are all weak. When Fisetin binds to AgNPs, SERS intensity of Fisetin significantly increases. From the datum and according to literatures,[29,30] the band at 1596 cm^{-1} involves C-C stretching vibration of ring B, C_2=C_3 stretching vibration and bending vibration -OH. The band at 1505 cm^{-1} involves C=O and C-C stretching vibration of ring B. The 1457 cm^{-1} band involves C=O stretching vibration of ring A-C. The 1355 cm^{-1} band involves C-C stretching vibration of ring A and C-OH bending vibration of ring A (7-OH) and C-OH bending vibration of ring C (3-OH). The 1252 cm^{-1} band involves C-C stretching vibration of ring A and ring A-C. The 1207 cm^{-1} band involves stretching vibration peak of C=O of ring A-C and C-OH bending vibration of ring A (7-OH). The 747 cm^{-1} band involves O=C-C-C torsion vibration peak of the ring A and ring A-C. The 475 cm^{-1} band involves C-C-C bending vibration peak of ring A and ring A-C. According to the SERS selection rules,[31] we consider that the -OH group in ring A and C=O group in ring C are close to the surface of silver nanoparticles. In contrast, the SERS spectrum of AgNPs-CTAB-Fisetin has the 883 cm^{-1} band, which involves C-C deformation of ring A, B and C. Compared to AgNPs- Fisetin, the Raman intensity of AgNPs-CTAB-Fisetin is decreased and many vibration peaks disappear. We think that AgNPs solubilize in CTAB micelles and form the micelles-capped AgNPs, the micelles hinder the direct interaction between AgNPs and Fisetin. In consequence, we further clarify the above hypothesis that Fisetin solubilizes in CTAB micelles and then combines with CTAB micelles-coated AgNPs.

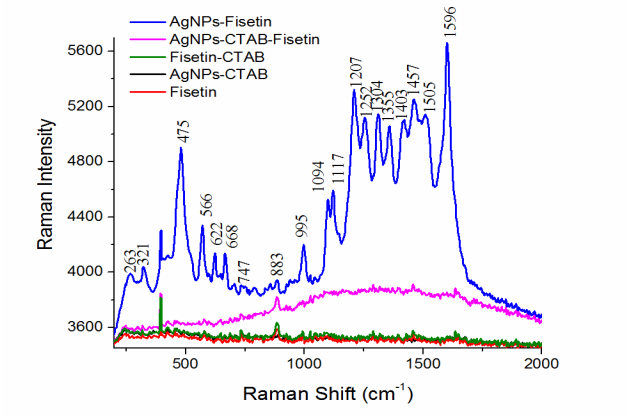

Fig. 6 Raman spectra of the system

Conditions: $C_{Fisetin}$: 5.0 × 10^{-5} moL L^{-1}, C_{CTAB}: 5.0 × 10^{-4} moL L^{-1}, C_{AgNPs}: 4.0 × 10^{-5} moL L^{-1}, Formic-NaOH : 2.0 × 10^{-2} moL L^{-1} (pH=5.2)

Fisetin exhibits two main absorption bands (Fig. 7), band I (about 357 nm) corresponds to the absorption of the cinnamoyl system (B-C ring) and band II (about 245 nm) corresponds to the absorption of the benzoyl system (A-C ring).[32,33] As shown in Fig. 6, CTAB micelles can cause red shift of the peak position of Fisetin to 362 nm. The absorbance of two bands all decrease. And the absorption profile of AgNPs-Fisetin is similar to Fisetin but the intensity decreases. As for CTAB-Fisetin, AgNPs can obviously increase its absorbance and exert almost no effects on its peak position. We believe that Fisetin molecules solubilize in CTAB micelles, and then combine with AgNPs in AgNPs-CTAB-Fisetin system.

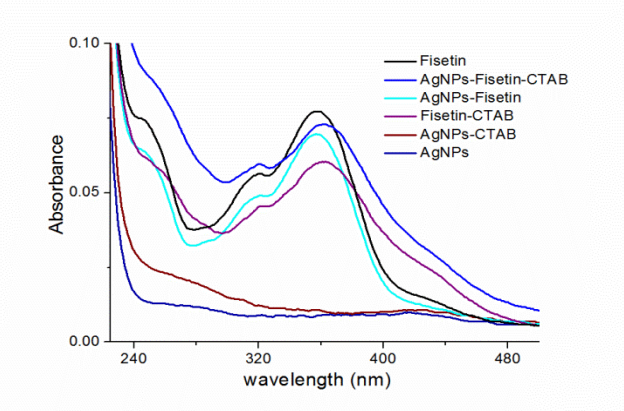

Fig. 7 Absorption spectra of the system

Conditions: $C_{Fisetin}$: 5.0 ×10^{-6} moL L^{-1}, C_{CTAB}: 5.0 × 10^{-4} moL L^{-1}, C_{AgNPs}: 4.0 × 10^{-6} moL L^{-1}, Formic-NaOH: 2.0 × 10^{-2} moL L^{-1} (pH=5.2)

The surface charges of nanoparticles were characterized by Zeta potential. The Zeta potentials of AgNPs, CTAB, AgNPs-CTAB, CTAB-Fisetin and AgNPs-CTAB-Fisetin were - 23.23 mV, + 83.76 mV, + 64.45 mV, + 53.96 mV and + 40.95 mV, respectively. We infer that Fisetin has anionic moiety, Fisetin molecules solubilize in CTAB micelles with positive charges by electrostatic attraction and hydrophobic interaction. The CTAB micelles neutralize negative charges AgNPs formation of the micelles-capped AgNPs. Based on fluorescence spectra and the above results, the possible mechanism of MEF of CTAB micelles-capped AgNPs is proposed as follow (Scheme-2): we believe that 7-hydroxyl deprotonation of Fisetin can occur in the optimal conditions. Fisetin molecules solubilize in Stern layer of CTAB micelles by electrostatic interaction and hydrophobic effect and then combine with CTAB micelles capped-AgNPs. The ESIPT reaction of Fisetin occurs under 365 nm excitation. The CTAB micelles provide the proper distance for Fisetin and AgNPs, leading to the obvious fluorescence enhancement of the system.

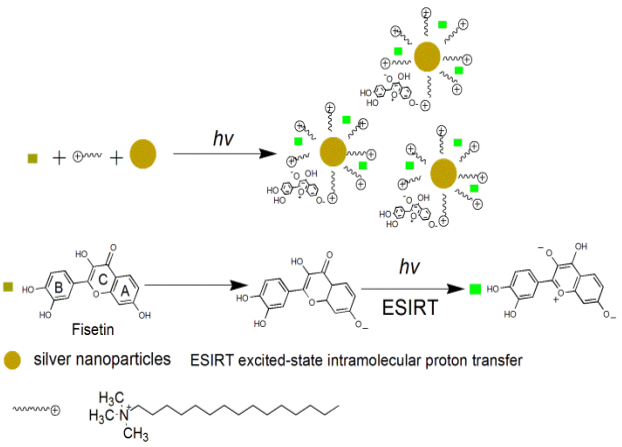

Scheme-2 Schematic diagram of mechanism of CTAB micelles-capped AgNPs enhance fluorescence of Fisetin

Conclusions

In summary, we proposed in situ synthesized cetyltrimethyl ammonium bromide micelles-capped silver nanoparticles for the determination of Fisetin. The detection limit (*S/N = 3*) is down to nmoL L^{-1}. Investigations of the interaction mechanisms of the system demonstrate that Fisetin molecules solubilize in cetyltrimethyl ammonium bromide micelles and then combine with silver nanoparticles coated by the micelles. In this work, the selective fluorescence response of Fisetin should be attributed to binding site of hydroxyl groups and the solubilization in cetyltrimethyl ammonium bromide micelles. The CTAB micelles provide the suitable distance between Fisetin and the surface of silver nanoparticles for metal-enhanced fluorescence, leading to the obvious fluorescence enhancement of the system.

Notes and references

Key Laboratory of Colloid and Interface Chemistry (Shandong University), Ministry of Education, School of Chemistry and Chemical Engineering, Shandong University, Jinan 250100, P. R. China
Corresponding author, Tel.:+86 53188365459; Fax: +86 53188564464; e-mail address: wux@sdu.edu.cn (X. Wu)

† Electronic Supplementary Information (ESI) available: [details of any supplementary information available should be included here]. See DOI: 10.1039/b000000x/

1 A-M. Alam，M. Kamruzzaman，S.H. Lee，Y.H. Kim，S.Y. Kim and G.M. Kim, *Microchim. Acta.*, 2012, **176**, 153–161.
2 P. Hua, L. Zheng, L. Zhan, J. Li, S. Zhen and H. Liu, *Anal. Chim. Acta.*, 2013, **787**, 239-245.
3 Y. Wang, Z. Li, H. Li, M. Vuki, D. Xu and H-Y. Chen, *Biosensors and Bioelectronics*, 2012, **32**, 76– 81.
4 H. Li, C-Y. Chen, X. Wei, W. Qiang, Z. Li and Q. Cheng , *Anal. Chem.*, 2012, **84**, 8656–8662.
5 J. Zhang, Y. Fu, M.H. Chowdhury and J.R. Lakowicz, *Nano. Lett.*, 2007, **7**, 2101-2107.
6 H. Li, W. Qiang, M. Vuki, D. Xu and H-Y. Chen, *Anal. Chem.*, 2011, **83**, 8945–8952.
7 J. Zhang, N. Ma, F. Tang, Q. Cui, F. He and L. Li, *ACS Appl. Mater. Interfaces.*, 2012, **4**,1747–1751.
8 B. Pahari, B. Sengupta, S. Chakraborty, B. Thomas, D. McGowan and P.K. Sengupta, *J. Photochem. Photobiol. B.*, 2013, **118**, 33–41.
9 G. Gutiérrez-Venegas and A. Contreras-Sánchez, *Mol. Biol. Rep.*, 2013, **40**, 477–485.
10 K.T. Howitz, K.J. Bitterman, H.Y. Cohen, D.W. Lamming, S. Lavu and J.G. Wood, *Nature*, 2003, **425**, 191–196.
11 I-J. Jo, G-S. Bae, S.B. Choi, D-G. Kim, J-Y. Shin and S-H. Seo, *European Journal of Pharmacology*, 2014, **737**, 149–158.
12 N. Khan, F. Afaq, D.N. Syed and H. Mukhtar, *Carcinogenesis*, 2008, **29**, 1049–1056.
13 D.N. Syed, F. Afaq, N. Maddodi, J.J. Johnson, S. Sarfaraz and A. Ahmad, *J. Invest. Dermatol.*, 2011, **131**, 1291–1299.
14 G.S. Prasath, S.I. Pillai and S.P. Subramanian, *European Journal of Pharmacology*, 2014, **740**, 248–254.
15 P Maher, T Akaishi and K Abe, Proc. Natl. Acad. Sci. USA., 2006, **103**, 16568–16573.
16 A. S. Roy, N.K. Pandey and S. Dasgupta, *Mol. Biol. Rep*., 2013, **40**, 3239–3253.
17 S. Xu, Y. Shao, K. Ma, Q. Cui, G. Liu and F. Wu, *Sensors Actuators B Chem.*, 2012, **171-172**, 666–671.
18 I. Novak, P. Janeiro, M. Seruga and A.M. Oliveira-Brett, *analytica. Chimica. acta*, 2008, **630**, 107–115.
19 F. Fang, J-M. Li, Q-H. Pan and W-D. Huang, *Food Chemistry*, 2007, **101**, 428-433.
20 L. Jiang, G. Fang, Y. Zhang, G. Cao and S. Wang, *J. Agric. Food Chem.*, 2008, **56**, 11571–11577.
21 D. Brondani, I.C. Vieira, C. Piovezan, J.M.R. da Silva, A. Neves and J. Dupont, *Analyst*, 2010, **135**, 1015-1022.
22 G.J. Volikakis and C.E. Efstathiou, *Talanta*, 2000, **51**, 775-785.
23 J. Zheng, X. Wu, M. Wang, D. Ran, W. Xu and J. Yang, *Talanta*, 2008, **74**, 526–532.
24 M. R. Guzzo, M. Uemi, P. M. Donate, S. Nikolaou, A. E.H. Machado and L. T. Okano, *J. Phys. Chem. A.*, 2006, **110**, 10545-10551.
25 A. Banerjee and P. K. Sengupta, *Chemical Physics Letters*, 2006, **424**, 379–386.
26 J.M. Herrero-Martinez, M. Sanmartin, M. Roses, E. Bosch, C. Rafols, Electrophoresis, 2005, 26,1886-1895.
27 G. Li, D. Zhu, Q. Liu, L. Xue and H. Jiang, Org. Lett., 2013, 15, 924–927.
28 S-j. Yu, J-b. Chao, Y-g. Sun, J-f. Liu and G-b. Jiang, *Environ. Sci. Technol.*, 2013, **47**, 3268–3274.
29 M. Wang, T. Teslova, F. Xu, T. Spataru, J. R. Lombardi and R. L. Birke, *J. Phys. Chem. C.*, 2007, **111**, 3038-3043.
30 J. M. Dimitri´Markovi´, Z. S. Markovi´ and D. Milenkovi´, S. Jeremi´, *Spectrochimica Acta Part A*, 2011, **83**,120–129.
31 S.M. Ansar, X. Li, S. Zou and D. Zhang, *J. Phys. Chem. Lett.*, 2012, **3**, 560–565.
32 B. Naseem, S.W.H. Shah, A. Hasan and S. S. Shah, *Spectrochimica Acta Part A*, 2010, **75**, 1341–1346.
33 W. Liu and R. Guo, *J. Colloid Interface Sci*, 2006, **302**, 625–632.